Mechanics of Materials 69 (2014) 195–203

Contents lists available at ScienceDirect

Mechanics of Materials

journal homepage: www.elsevier.com/locate/mechmat

Stress-function variational approach to the interfacial stresses and progressive cracking in surface coatings

Xiang-Fa Wu *, Robert A. Jenson, Youhao Zhao

Department of Mechanical Engineering, North Dakota State University, Fargo, ND 58108, USA

ARTICLE INFO

Article history:
Received 21 December 2012
Received in revised form 1 October 2013
Available online 25 October 2013

Keywords:
Surface coatings
Progressive cracking
Free-edge stresses
Fracture criterion

ABSTRACT

Surface coatings are broadly used in cutting tools, protective surface, and recently developed flexible electronics. This paper provides a simple semi-analytic strain energy approach to analysis of the interfacial stresses and progressive cracking in hard coatings subjected to mechanical and thermomechanical loads. The problem is formulated within the framework of linear elastic fracture mechanics (LEFM). The free-edge stresses in cracked coating layers are determined by means of an efficient semi-analytic stress-function variational method formulated by the authors recently. Criterion for progressive cracking in the coating layers is established in the sense of energy conservation. The crack spacing is determined as a function with respect to the geometries, material properties, and external loads. Dependencies of the free-edge stresses and crack spacing upon the geometries and material parameters of the coating system as well as external loads are demonstrated. Numerical results show that given a coating system, the threshold load increases rapidly with the decrease of crack spacing; the thicker and stiffer the coating layer is, the easier the progressive cracking is. A universal scaling number on progressive cracking is obtained. The model is also validated by the results in the literature. The present phenomenological model is applicable for scaling analysis of cracking tolerance of surface coatings, data reduction of coating experiments, design of property-tailorable surface coating systems, etc.

1. Introduction

A number of surface crack patterns have been observed in layered structures in nature and engineered materials such as dried mud, weathered stone, and surface coatings (Bažant, 1986; Bai et al., 2000; Bai and Pollard, 2000; Xia and Hutchinson, 2000; Leung et al., 2001). In nature, significant cracking events are related to the surface where drying or weathering of the surface layers plays a dominate role. For instance, water evaporation in a drying mud induces a large residual tensile strain while the substrate restrains the free shrinking of the surface layer. In consequence, surface cracking takes place when the residual tensile stress of the surface layer reaches its strength (Hutchinson and Suo, 1992; Colina and Roux, 2000; Neda et al., 2002; Lee and Routh, 2004; Mal et al., 2005; Bohn et al., 2005a,b; Mizuguchi et al., 2005; Dufresne et al., 2006; Nakahara and Matsuo, 2006; Singh and Tirumkudulu, 2007). In parallel, engineered surface coatings have been widely used for the purpose of anticorrosion, solid lubrication, thermal barriers of gas turbines. Surface coatings typically belong to brittle thin-film on compliant substrate (e.g., diamond coating on alloy tools, silicon islands on compliant polymer films). Subjected to mechanical or thermomechanical loads, surface cracking or buckling delamination of the brittle hard coating layers may appear in these systems (Mei et al., 2011). In the view of fracture mechanics, the initiation and growth of surface cracks is dominated by the stress state near crack tip and the crack growth criterion. The former relies on an accurate stress analysis while the latter can be identified through controlled fracture test and formulation of robust fracture criterion.

* Corresponding author. Tel.: +1 701 231 8836; fax: +1 701 231 8913.
E-mail address: xiangfa.wu@ndsu.edu (X.-F. Wu).

0167-6636/$ - see front matter Crown Copyright © 2013 Published by Elsevier Ltd. All rights reserved.
http://dx.doi.org/10.1016/j.mechmat.2013.10.004

To date, quite a few efficient mechanics models have been formulated for prediction of cracking in surface coatings (Hutchinson and Suo, 1992; Kim and Nairn, 2000a,b; Evans et al., 2001; Mishnaevsky and Gross, 2005; and Refs. therein). Among these, the simplest crack model was based on Cox's shear-lag concept (Cox, 1952). In-depth studies have been further performed with the principle of energy conservation (Thouless, 1990; Hong et al., 1997; Kim and Nairn, 2000a,b; Wu et al., 2008), in which the strain energy requested to generate the crack is equal to the difference of strain energy of the system before and after cracking, and the crack spacing is limited by the strain energy available in the system (Bai et al., 2000). In classic models of progressive cracking in surface coatings, the corresponding strain energy was usually calculated according to the elementary beam theory and other reduced semi-analytic techniques. Yet, these oversimplified models typically yield the incompatible stress fields that do not satisfy the traction boundary conditions (BCs) at crack tips. By refining these models, it is possible to take into more accurate estimate of the high interfacial stresses near the crack tips while maintaining the advantages of analytic models. Therefore, in this study we are going to formulate a simple semi-analytic strain energy method to analyze the interfacial stresses and progressive cracking in surface coatings within the framework of linear elastic fracture mechanics (LEFM). The free-edge stresses in the cracked coating layers are determined by means of a stress-function variational method formulated by the authors recently (Wu and Jenson, 2011; Wu and Zhao, 2013). Criterion of progressive cracking in the coating layers is established according to the principle of energy conservation. The crack spacing is determined as a function of geometries, material properties, and external loads. Dependencies of the free-edge stresses and crack spacing upon the geometrical and material parameters of the coating system as well as the external loads are demonstrated via numerical experimentation. Discussions of the phenomenological failure mechanisms, parameter dependencies, and potential applications are further made. Conclusion of the study is addressed in consequence.

2. Problem formulation and solution

2.1. Stress field and strain energy of a surface-cracked coating system

In general, progressive cracking in surface coating is a complex three-dimensional (3D) failure phenomenon. To simplify the process, we consider a reduced two-dimensional (2D) *plane-strain* case such that the crack penetrates the coating surface in the transverse direction and assume that no residual stresses exist in the initial load-free state at a reference temperature. The temperature change in the coating system is treated to be uniform. Besides, the substrate and coating layers are considered as isotropic, linear thermoelastic solids. Thus, for a compliant substrate layer coated with a hard (brittle) surface layer subjected to axial tension, transverse bending, and/or temperature change to some extent, periodic cracks may appear in the coating layer as illustrated in Fig. 1.

By assuming idealized periodicity of the surface cracking, a representative element can be adopted as shown in Fig. 2(a) for the purpose of analyzing the interfacial stress and failure in the coating layers. Such a representative element can be treated as a single-sided strap joint. An improved analysis of the stress field and strain energy of such a joint has been made recently by using a stress-function variational method (Wu and Jenson, 2011). This method is adopted herein for analysis of progressive cracking in the surface layer. We start with the stress analysis of a single-sided strap joint consisting of a slender substrate layer and a slender coating layer (Fig. 2(a)). By adopting the same notations by Wu and Jenson (2011), the thicknesses

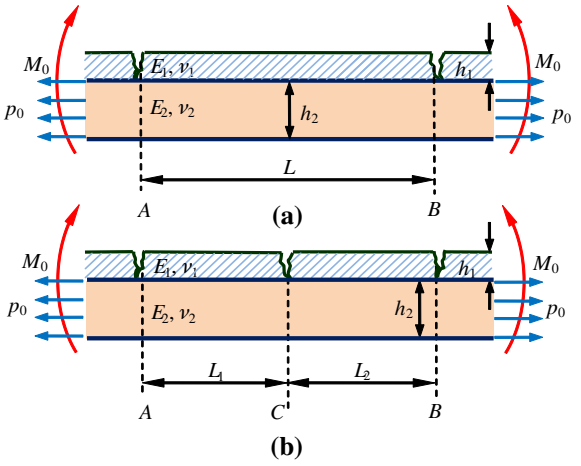

Fig. 1. (a) Through-thickness cracking in the coating layer of a brittle thin-film/substrate system; (b) formation of a secondary crack at a new locus between adjacent cracks.

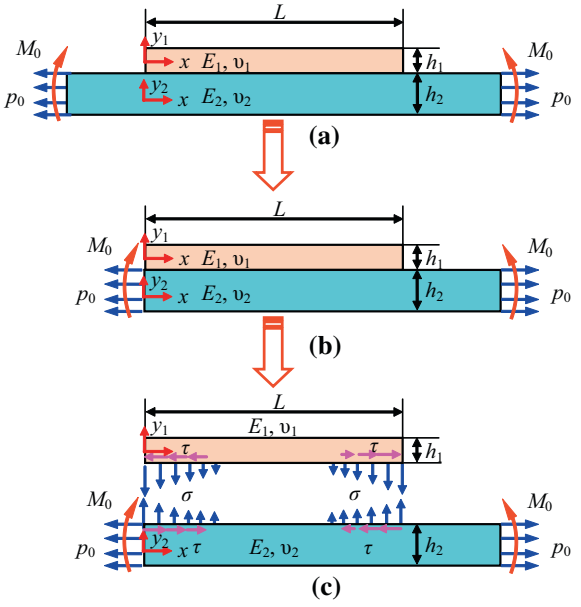

Fig. 2. Schematic of a single-sided strap joint as a mechanics model of a cracked surface coating system: (a) The joint consists of a slender coating layer bonded to a slender substrate layer, (b) reduced traction boundary conditions, and (c) schematic interfacial shear and normal stresses.

of the coating and substrate layers are designated as h_1 and h_2, respectively; the length of the representative element is L. The coordinate systems are defined as follows. The x-coordinate is set with the origin located at the left end of the representative segment and directs along the layer axis; y_1 and y_2 are the ordinates with the corresponding origins located at the centroids of cross-sections of the coating and substrate layers, respectively. In this study, a general loading condition will be considered such that the substrate layer is treated under the combined action of a uniform tensile stress p_0, a pair of bending moments, and a uniform temperature change ΔT from the reference temperature of thermal stress-free state. Fig. 2(b) specifies the traction BCs of the left end. Due to mismatch of the material properties across the bonding line (i.e., Poisson's ratios and coefficients of thermal expansion), high interfacial normal (peeling) and shear stresses are triggered near the ends of the coating layer as illustrated in Fig. 2(c). Such high interfacial stresses are responsible for the debonding failure of the surface coating system. In addition, for the convenience of derivation, parameters and variables with subscripts 1 and 2 are attached to those of the coating and substrate layers, respectively.

For such a coating system, the inplanar shear and normal stresses on the interface are considered as two independent unknown functions, i.e., the interfacial shear stress τ and interfacial normal (peeling) stress σ:

$$\tau = f(x) \text{ and } \sigma = g(x). \tag{1}$$

With the assumption that the axial stresses in the coating and substrate layers follow a linear distribution similar to those in the elementary *Euler–Bernoulli beam* theory while the shear and lateral normal stresses in the layers exactly satisfy the stress equilibrium equations in 2D elasticity (Timoshenko and Goodier, 1951; Wu and Jenson, 2011), the entire stress field in the coating and substrate layers can be expressed in terms of the interfacial stress functions f and g as follows.

(1) Stress field in the coating layer

$$\sigma_{xx}^{(1)} = -\frac{1}{h_1}\int_0^x f(\xi)d\xi + \frac{12y_1}{h_1^3}\left[\int_0^x\int_0^\xi g(\varsigma)d\varsigma d\xi + \frac{h_1}{2}\int_0^x f(\xi)d\xi\right], \tag{2}$$

$$\tau_{y_1x}^{(1)} = -\frac{1}{h_1}\left[\left(\frac{h_1}{2}-y_1\right)-\frac{3}{h_1}\left(\frac{h_1^2}{4}-y_1^2\right)\right]f(x) + \frac{6}{h_1^3}\left(\frac{h_1^2}{4}-y_1^2\right)\int_0^x g(\xi)d\xi, \tag{3}$$

$$\sigma_{y_1y_1}^{(1)} = -\frac{1}{h_1}\left\{\frac{h_1}{2}\left(\frac{h_1}{2}-y_1\right)-\frac{1}{2}\left(\frac{h_1^2}{4}-y_1^2\right) -\frac{3}{h_1}\left[\frac{h_1^2}{4}\left(\frac{h_1}{2}-y_1\right)-\frac{1}{3}\left(\frac{h_1^3}{8}-y_1^3\right)\right]\right\}f'(x) + \frac{6}{h_1^3}\left[\frac{h_1^2}{4}\left(\frac{h_1}{2}-y_1\right)-\frac{1}{3}\left(\frac{h_1^3}{8}-y_1^3\right)\right]g(x). \tag{4}$$

(2) Stress field in the substrate layer

$$\sigma_{xx}^{(2)} = p_0 + \frac{1}{h_2}\int_0^x f(\xi)d\xi - \frac{12y_2}{h_2^3}\left[M_0 + \int_0^x\int_0^\xi g(\varsigma)d\varsigma d\xi - \frac{h_2}{2}\int_0^x f(\xi)d\xi\right], \tag{5}$$

$$\tau_{y_2x}^{(2)} = -\frac{1}{h_2}\left[\left(y_2+\frac{h_2}{2}\right)+\frac{3}{h_2}\left(y_2^2-\frac{h_2^2}{4}\right)\right]f(x) + \frac{6}{h_2^3}\left(y_2^2-\frac{h_2^2}{4}\right)\int_0^x g(\xi)d\xi, \tag{6}$$

$$\sigma_{y_2y_2}^{(2)} = \left\{\frac{1}{h_2}\left[\frac{1}{2}\left(y_2^2-\frac{h_2^2}{4}\right)+\frac{h_2}{2}\left(y_2+\frac{h_2}{2}\right)\right] +\frac{3}{h_2^2}\left[\frac{1}{3}\left(y_2^3+\frac{h_2^3}{8}\right)-\frac{h_2^2}{4}\left(y_2+\frac{h_2}{2}\right)\right]\right\}f'(x) - \frac{6}{h_2^3}\left[\frac{1}{3}\left(y_2^3+\frac{h_2^3}{8}\right)-\frac{h_2^2}{4}\left(y_2+\frac{h_2}{2}\right)\right]g(x). \tag{7}$$

The interfacial stress functions f and g satisfy a system of two coupled 4th-order ordinary differential equations (ODEs) of constant coefficients (Wu and Jenson, 2011):

$$[\mathrm{A}]\{\Phi^{(IV)}\} + [\mathrm{B}]\{\Phi''\} + [\mathrm{C}]\{\Phi\} + \{\mathrm{D} = \{0\}, \tag{8}$$

where

$$\{\Phi\} = \{F(\xi), G(\xi)\}^T, \tag{9}$$

$$F(\xi) = F(x/h_2) = -\frac{1}{p_0h_2}\int_0^x f(\zeta)d\zeta, \tag{10a}$$

$$G(\xi) = G(x/h_2) = \frac{1}{p_0h_2^2}\int_0^x\int_0^\zeta g(\eta)d\eta d\zeta, \tag{10b}$$

$$[\mathrm{A}] = [\mathrm{A}]^{\mathrm{T}} = \begin{bmatrix} A_{11} & A_{12} \\ A_{12} & A_{22}\end{bmatrix}, \tag{11a}$$

$$[\mathrm{B}] = [\mathrm{B}]^{\mathrm{T}} = \begin{bmatrix} B_{11} & B_{12} \\ B_{12} & B_{22}\end{bmatrix}, \tag{11b}$$

$$[\mathrm{C}] = [\mathrm{C}]^{\mathrm{T}} = \begin{bmatrix} C_{11} & C_{12} \\ C_{12} & C_{22}\end{bmatrix}, \tag{11c}$$

$$\{D\} = \{D_1, D_2\}^T, \tag{11d}$$

and the elements of [A], [B], [C], and {D} are given by Wu and Jenson (2011) and listed in Appendix. The solution to (8) can be expressed as

$$\{\Phi\} = \sum_{k=1}^{4}[c_k\{\Psi_0^k\}\exp(\lambda_k\xi) + d_k\{\Psi_0^k\}\exp(-\lambda_k\xi)] + \{\Phi_0\}. \tag{12}$$

In the above, λ_k and $\{\Psi_0^k\}$ (k = 1–4) are respectively the kth eigenvalue and its corresponding eigenvector of the characteristic equation with respect to (8):

$$\lambda^4[A]\{\Psi_0\}+\lambda^2[B]\{\Psi_0\}+[C]\{\Psi_0\}=\{0\}. \tag{13}$$

c_k and d_k (k = 1–4) are the unknown coefficients to be determined satisfying all the traction BCs of the cover and substrate layers (Wu and Jenson, 2011). $\{\Phi_0\}$ is the particular solution to (8):

$$\{\Phi_0\}=-[C]^{-1}\{D\}. \tag{14}$$

Once $\{\Phi\}$ is determined from (12), f and g can be obtained from (10a) and (10b) as

$$f(x)/p_0=\sum_{k=1}^{4}c_k\Psi_0^{k,1}\lambda_k\exp(\lambda_k x/h_2)-\sum_{k=1}^{4}d_k\Psi_0^{k,1}\lambda_k\exp(-\lambda_k x/h_2), \tag{15}$$

$$g(x)/p_0=\sum_{k=1}^{4}c_k\Psi_0^{k,2}\lambda_k^2\exp(\lambda_k x/h_2)+\sum_{k=1}^{4}d_k\Psi_0^{k,2}\lambda_k^2\exp(-\lambda_k x/h_2). \tag{16}$$

In addition, the strain energy of the coating system per unit longitudinal length can be expressed as

$$e=\int_{-h_1/2}^{h_1/2}\left\{\frac{1}{2}[\sigma_{xx}^{(1)}\varepsilon_{xx}^{(1)}+\sigma_{yy}^{(1)}\varepsilon_{yy}^{(1)}]+\frac{(1+\upsilon_1)}{E_1}[\tau_{xy_1}^{(1)}]^2\right\}dy_1+\int_{-h_2/2}^{h_2/2}\left\{\frac{1}{2}[\sigma_{xx}^{(2)}\varepsilon_{xx}^{(2)}+\sigma_{yy}^{(2)}\varepsilon_{yy}^{(2)}]+\frac{(1+\upsilon_2)}{E_2}[\tau_{xy_2}^{(2)}]^2\right\}dy_2. \tag{17}$$

By utilizing the governing ODE (8), the strain energy density (17) can be expressed as

$$e=\frac{1}{2}\{\Phi\}^T\{D\}\frac{p_0^2h_2}{E_1/(1-\upsilon_1^2)}+\frac{6}{[E_2/(1-\upsilon_2^2)]h_2^3}M_0^2+\frac{h_2}{2E_2/(1-\upsilon_2^2)}p_0^2+\frac{(1+\upsilon_2)\alpha_2h_2}{2}\Delta Tp_0. \tag{18}$$

Substitution of (12) into (18) leads to

$$e(\xi)=\frac{1}{2}\sum_{k=1}^{4}[c_k\{\Psi_0^k\}^T\{D\}\exp(\lambda_k\xi)+d_k\{\Psi_0^k\}^T\{D\}\exp(-\lambda_k\xi)]\frac{p_0^2h_2}{E_1/(1-\upsilon_1^2)}-\frac{1}{2}\{D\}^T[C]^{-1}\{D\}\frac{p_0^2h_2}{E_1/(1-\upsilon_1^2)}+\frac{6}{[E_2/(1-\upsilon_2^2)]h_2^3}M_0^2+\frac{h_2}{2E_2/(1-\upsilon_2^2)}p_0^2+\frac{(1+\upsilon_2)\alpha_2h_2}{2}\Delta Tp_0. \tag{19}$$

In expression (19), the first term is the extra strain energy density due to localized stress concentration induced by the cracks (free ends) which is a function with respect to the coating thickness, elastic properties and locus; the rest is the strain energy density of an initial crack-free coating and substrate layers denoted as e_0, i.e.,

$$e_0=-\frac{1}{2}\{D\}^T[C]^{-1}\{D\}\frac{p_0^2h_2}{E_1/(1-\upsilon_1^2)}+\frac{6}{[E_2/(1-\upsilon_2^2)]h_2^3}M_0^2+\frac{h_2}{2E_2/(1-\upsilon_2^2)}p_0^2+\frac{(1+\upsilon_2)\alpha_2h_2}{2}\Delta Tp_0. \tag{20}$$

In addition, the strain energy density corresponding to a coating system with a single crack in the coating layer (left-half $\xi>0$) is

$$e_\infty(\xi)=\frac{1}{2}\sum_{k=1}^{4}d_k\{\Psi_0^k\}^T\{D\}\exp(-\lambda_k\xi)\frac{p_0^2h_2}{E_1/(1-\upsilon_1^2)}-\frac{1}{2}\{D\}^T[C]^{-1}\{D\}\frac{p_0^2h_2}{E_1/(1-\upsilon_1^2)}+\frac{6}{[E_2/(1-\upsilon_2^2)]h_2^3}M_0^2+\frac{h_2}{2E_2/(1-\upsilon_2^2)}p_0^2+\frac{(1+\upsilon_2)\alpha_2h_2}{2}\Delta Tp_0, \tag{21}$$

where λ_k (k = 1–4) are the four eigenvalues with positive real parts, d_k (k = 1–4) are determined to satisfy the traction BCs, which leads to a system of four linear algebraic equations:

$$\sum_{k=1}^{4}d_k\Psi_0^{k,1}=-\Phi_0^{(1)}, \tag{22a}$$

$$\sum_{k=1}^{4}d_k\lambda_k\Psi_0^{k,1}=0, \tag{22b}$$

$$\sum_{k=1}^{4}d_k\Psi_0^{k,2}=-\Phi_0^{(2)}, \tag{22c}$$

$$\sum_{k=1}^{4}d_k\lambda_k\Psi_0^{k,2}=0. \tag{22d}$$

The above system of four linear algebraic equations is the reduced version of the case of bonded strip joints (Wu and Jenson, 2011).

2.2. Progressive cracking analysis

2.2.1. Critical loading and temperature change for appearance of first cracking in surface coating layers

Within the framework of linear elastic fracture mechanics (LEFM), the criterion of through-thickness cracking in the coating layer is formulated such that subjected to constant loads (M_0 or p_0) or temperature change ΔT, the strain energy increase ΔU due to cracking is equal to the strain energy release $\Delta\Gamma$:

$$\Delta U=\Delta\Gamma=G_ch_1, \tag{23}$$

where G_c is the critical strain energy release rate (ERR) of the surface crack in the coating layer. In the present phenomenological approach, we only consider the strain energy variation before and after the through-thickness cracking in the coating layer. By using the strain energy densities (20) and (21), the cracking criterion (23) for the occurrence of the first cracking is

$$G_ch_1=2\int_0^{+\infty}(e_\infty(\xi)-e_0)d\xi, \tag{24}$$

which can be reduced as

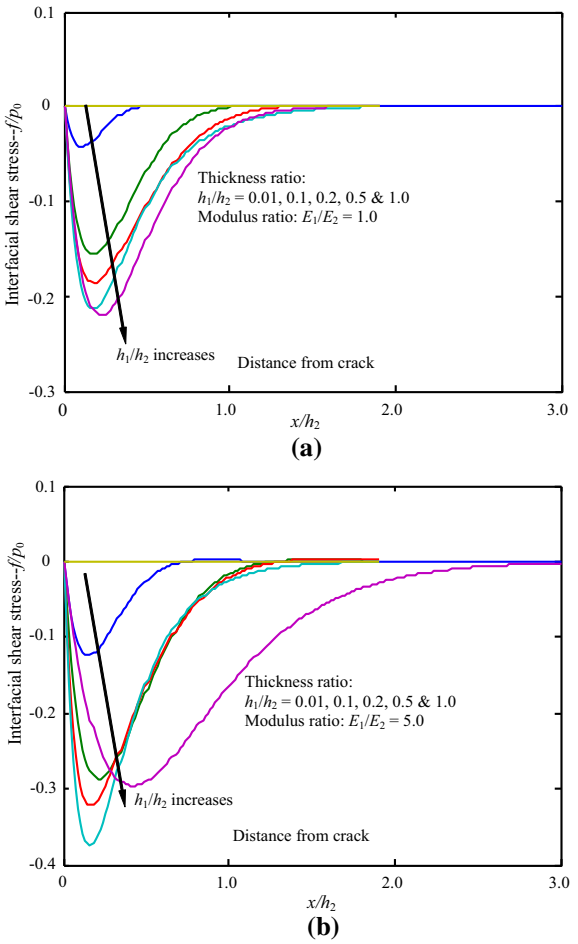

Fig. 3. Variation of the dimensionless interfacial shear stresses in a single-cracked hard coating system at five thickness ratios (h_1/h_2 = 0.01, 0.02, 0.05, 0.1 and 0.2): (a) modulus ratios E_1/E_2 = 1.0 and (b) E_1/E_2 = 5.0.

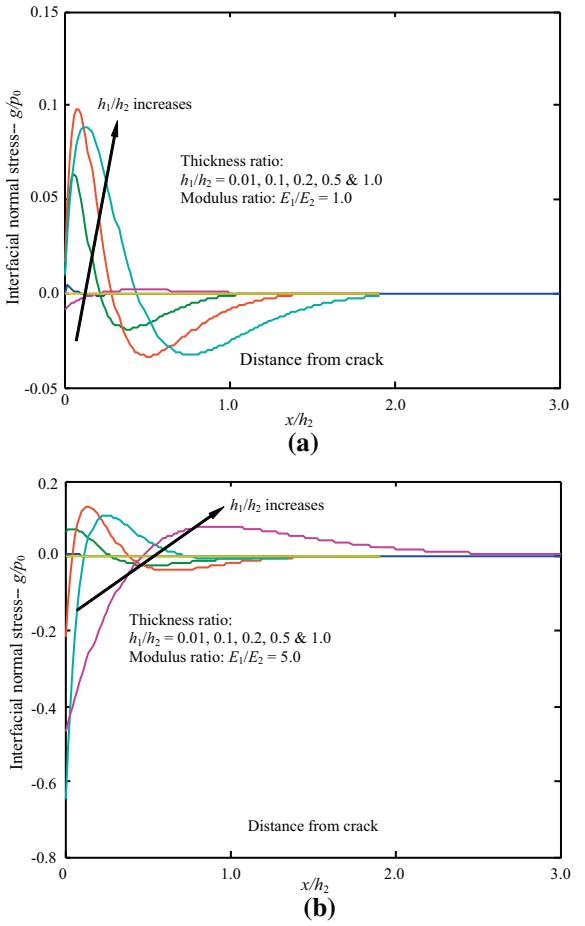

Fig. 4. Variation of the dimensionless interfacial normal stresses in a single-cracked hard coating system at five thickness ratios (h_1/h_2 = 0.01, 0.02, 0.05, 0.1 and 0.2): (a) modulus ratio E_1/E_2 = 1.0 and (b) E_1/E_2 = 5.0.

$$\sum_{k=1}^{4} d_k \lambda_k^{-1} \{\Psi_0^k\}^T \{D\} \frac{p_0^2 h_2^2}{E_1/(1-\upsilon_1^2)} = G_c h_1. \tag{25}$$

The left side of (25) has a quadratic term with respect with p_0, M_0 and ΔT:

$$\sum_{k=1}^{4} d_k \lambda_k^{-1} \{\Psi_0^k\}^T \{D\} \frac{p_0^2 h_2}{E_1/(1-\upsilon_1^2)} = A_{pp} p_0^2 + A_{MM} M^2 + A_{TT} (\Delta T)^2 + A_{pM} p_0 M + A_{pT} p_0 \Delta T + A_{MT} M \Delta T, \tag{26}$$

where A_{pp}, A_{MM}, A_{TT}, A_{pM}, and A_{MT} are coefficients relating the geometries and material properties of the coating system. Relation (26) is the general strain energy criterion for the appearance of first cracking subjected to combined tension, bending and temperature change. This criterion can also be used for a reduced single loading case such as temperature-induced surface cracking.

2.2.2. Progressive cracking and crack spacing in surface coating layers

To study the progressive cracking in a surface coating layer, it is desirable to determine the crack density as a function with respect to the external loads and temperature change. Consider that an external load (e.g., a tensile force, bending moment, or temperature change) gradually increases its magnitude till it reaches the threshold value, at which the next cracking appears between two adjacent cracks with spacing L (see Fig. 1). It is reasonable to first consider the next cracking at an arbitrary locus C between AB. According to the strain energy criterion (23) for surface cracking, it reads

$$G_c h_1 = \int_0^{s_1} e(\xi) d\xi + \int_0^{s_2} e(\xi) d\xi - \int_0^{s} e(\xi) d\xi, \tag{27}$$

where $s_1 = L_1/h_2$, $s_2 = L_2/h_2$, $s = L/h_2$ ($s = s_1 + s_2$), and $e(\xi)$ is given by (19). The three integrals in (27) can be expressed explicitly:

$$G_c h_1 = \Pi_1 + \Pi_2 - \Pi_3, \tag{28}$$

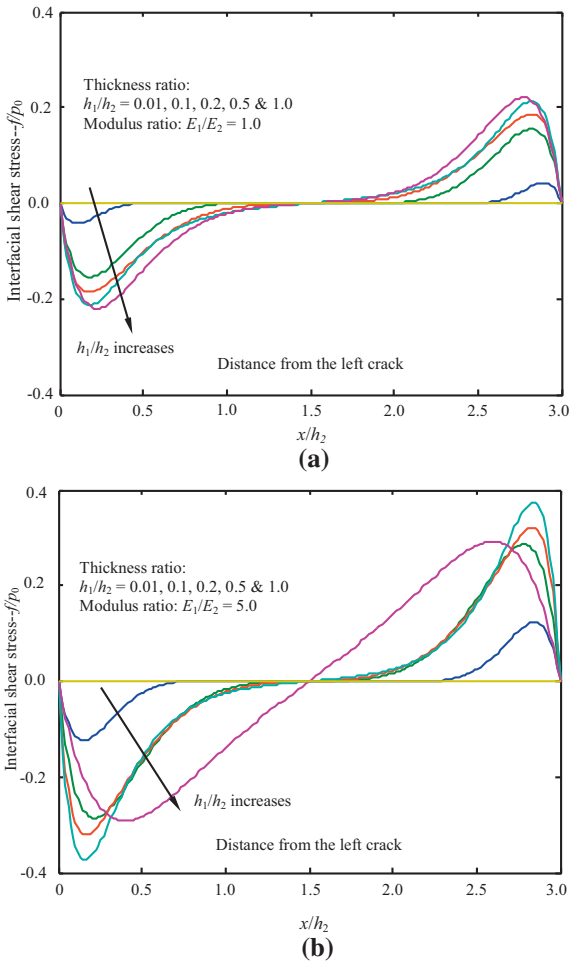

Fig. 5. Variation of the dimensionless interfacial shear stresses in a hard coating system with periodic surface cracks at five thickness ratios (h_1/h_2 = 0.01, 0.02, 0.05, 0.1 and 0.2): (a) modulus ratio E_1/E_2 = 1.0 and (b) E_1/E_2 = 5.0.

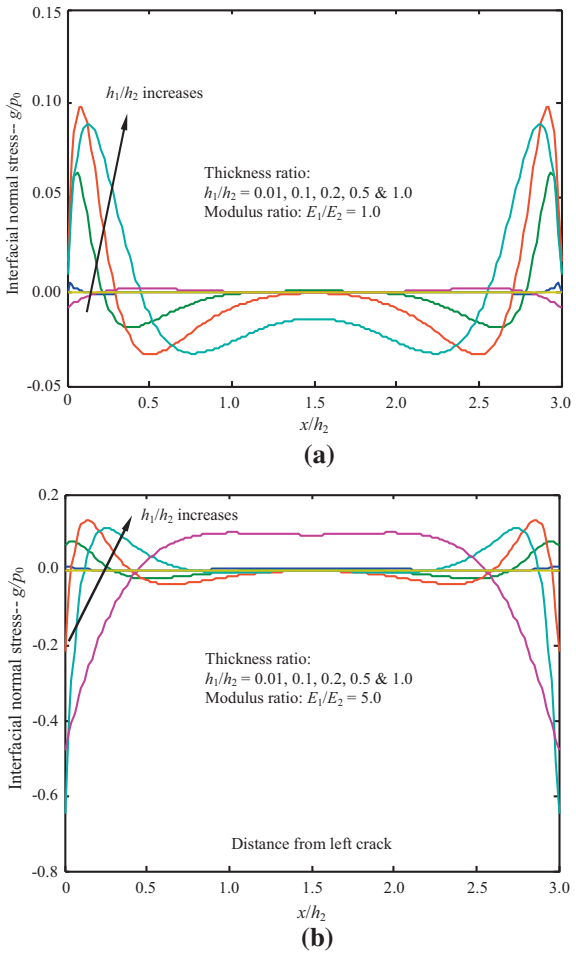

Fig. 6. Variation of the dimensionless interfacial normal stresses in a hard coating system with periodic surface cracks at five thickness ratios (h_1/h_2 = 0.01, 0.02, 0.05, 0.1 and 0.2): (a) modulus ratio E_1/E_2 = 1.0 and (b) E_1/E_2 = 5.0.

where

$$\Pi_1 = \left\{\sum_{k=1}^{4} \sinh\frac{\lambda_k s_1}{2}\left[c_k\lambda_k^{-1}\exp\left(\frac{\lambda_k s_1}{2}\right)\{\Psi_0^k\}^T + d_k\lambda_k^{-1}\exp\left(\frac{-\lambda_k s_1}{2}\right)\{\Psi_0^k\}^T\right]\right\}\{D\}\frac{p_0^2 h_2^2}{E_1/(1-\upsilon_1^2)}, \tag{29a}$$

$$\Pi_2 = \left\{\sum_{k=1}^{4} \sinh\frac{\lambda_k s_2}{2}\left[c_k\lambda_k^{-1}\exp\left(\frac{\lambda_k s_2}{2}\right)\{\Psi_0^k\}^T + d_k\lambda_k^{-1}\exp\left(\frac{-\lambda_k s_2}{2}\right)\{\Psi_0^k\}^T\right]\right\}\{D\}\frac{p_0^2 h_2^2}{E_1/(1-\upsilon_1^2)}, \tag{29b}$$

$$\Pi_3 = \left\{\sum_{k=1}^{4} \sinh\frac{\lambda_k s}{2}\left[c_k\lambda_k^{-1}\exp\left(\frac{\lambda_k s}{2}\right)\{\Psi_0^k\}^T + d_k\lambda_k^{-1}\exp\left(\frac{-\lambda_k s}{2}\right)\{\Psi_0^k\}^T\right]\right\}\{D\}\frac{p_0^2 h_2^2}{E_1/(1-\upsilon_1^2)}. \tag{29c}$$

In the above, coefficients c_k and d_k (k = 1–4) in (29a), (29b), (29c) are the same as given in (12) with $L/h_2 = s_1$, s_2 and s, respectively.

For a specified single load or combined loads with constant ratio, relation (28) determines the threshold loads. Without loss of generality, the locus C of next cracking can be assumed to be a stochastic variable. In this case, it is favorable to introduce a probability density function p to describe the site of the next cracking. The expected value of the external threshold load P_c (either tensile traction p_0, bending moment M_0, or uniform temperature change ΔT) to induce the next cracking in the coating layer which already contains cracks with the crack density d (=1/L) is.

$$E[P_c(s)] = h_2\int_0^s p(\xi)P_c(\xi)d\xi. \tag{30}$$

The choice of the probability density function is crucial to determine the mean threshold load $E[P_c(s)]$ (Wu et al., 2008).

3. Numerical examples and discussions

3.1. Interfacial stresses in cracked surface coatings

Within the framework of the refined beam theory above, the explicit solutions to interfacial shear and normal stresses in a coating system are the same as those of bonded strip joints. In the special case of a single through-thickness crack in a coating layer, the corresponding interfacial shear and normal stresses right to the surface crack can be determined by (12) with $c_k = 0$ ($k = 1$–4) and d_k ($k = 1$–4). The latter can be determined by solving the set of linear algebraic equations in (22a), (22b), (22c), (22d).

In the view of failure and durability analysis of a coating system, it is useful to examine the effects of geometric parameters and material properties on the stress distribution in the system. To illustrate these effects, as an example, we consider a hard coating system is loaded with a constant tensile traction p_0 and a bending moment M_0. The loads p_0 and M_0 ensure no transverse deflection (i.e., uniaxial tension) prior to cracking and maintain the same loading configuration after surface cracking. Figs. 3 and 4 plot the variations of the dimensionless interfacial shear and normal stresses against the thickness ratio at two modulus ratios (Jenson, 2011). A few features can be captured through comparison of the stress results shown in these diagrams as follows. Both interfacial shear and normal stresses increase with increasing Young's modulus of the coating layer relative to the substrate (i.e., modulus ratio). In addition, the modulus ratio can appreciably influence the distribution of the interfacial stresses: when $E_1/E_2 = 1.0$, these stresses are localized within the domain $\sim 1.5h_2$; however, when $E_1/E_2 = 5.0$, the stress field spreads to the domain with the interval of $\sim 2.5h_2$.

In addition, in the case of periodic cracks in a coating system subjected to external loads as specified above, the interfacial shear and normal stresses between two adjacent cracks with spacing L are plotted against the dimensionless distance from the left crack with varying thickness and modulus ratios in Figs. 5 and 6, respectively. Similar to those predicted in the single crack model above, Figs. 5 and 6 indicate that the larger Young's modulus and coating thickness results in the higher magnitude of interfacial shear and normal stresses. Thus, it can be concluded that decreasing the effective stiffness of the coating layer (e.g., the Young's modulus or layer thickness) with respect

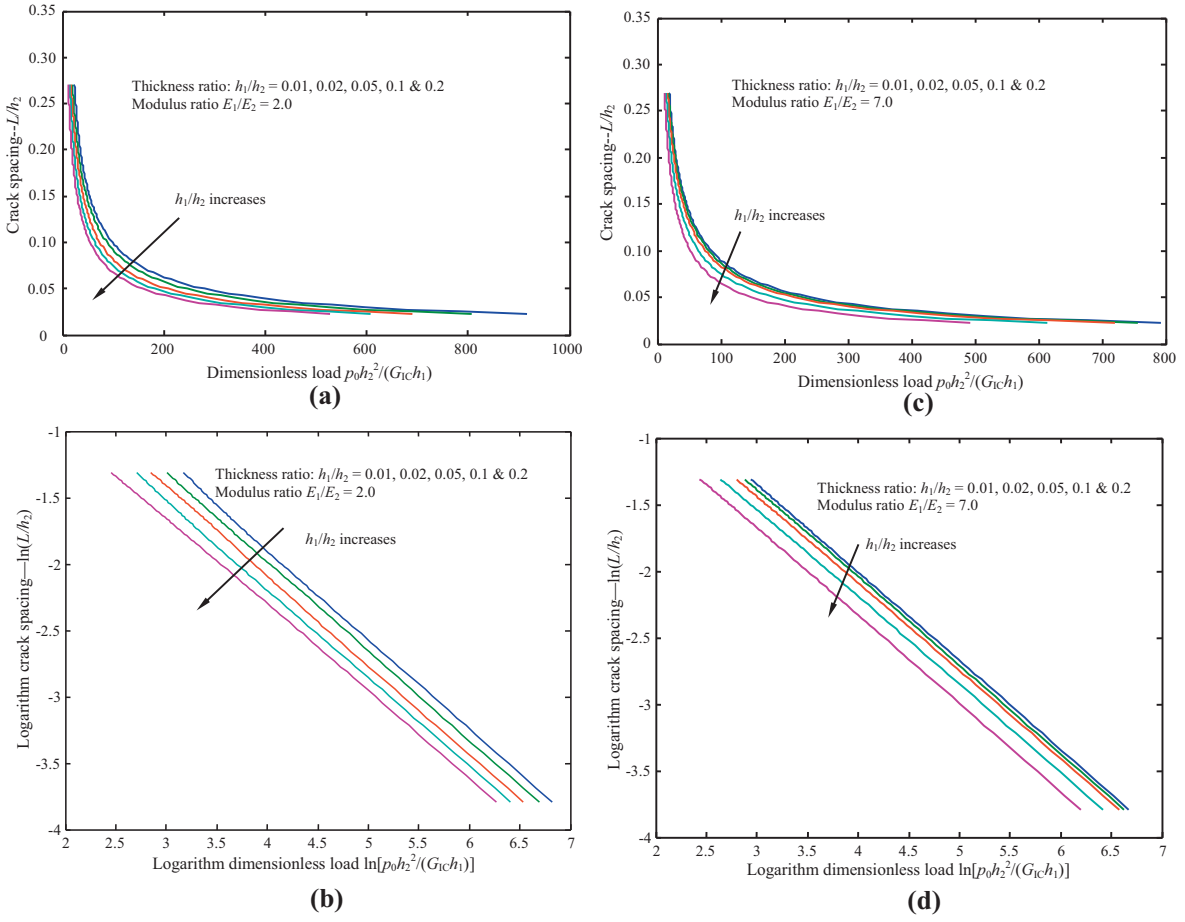

Fig. 7. Variation of the dimensionless crack spacing vs. the dimensionless threshold load at five thickness ratios (h_1/h_2 = 0.01, 0.02, 0.05, 0.1 and 0.2): (a) modulus ratios E_1/E_2 = 2.0, (*b*) plot of (a) in logarithm scale, (c) E_1/E_2 = 7.0, (d) plot of (c) in logarithm scale,

to the substrate can suppress the magnitude of the interfacial stresses.

3.2. Crack density in hard coating layers

Now let us consider the progressive cracking phenomenon in hard coating systems. For a gradually increasing external load (e.g., a tensile traction, bending moment, or temperature change), the initial cracking occurs in the coating layer once the criterion (24) is reached. After initial cracking, progressive cracking commences with the growing loads according to (28). Herein, variation of the dimensionless crack spacing with the dimensionless critical load $p_0h_2^2/G_ch_1$ is considered in the case of uniaxial tension prior to single cracking (i.e., constant axial traction) as studied in the above section. The critical load is taken to be the predicted value corresponding to the next cracking that is assumed to occur equidistant from the existing cracks at a spacing L/h_2 [Eq. (27) with $L_1 = L_2$]. Fig. 7 plots the dimensionless crack spacing over the dimensionless critical load at five thickness ratios (h_1/h_2 = 0.01, 0.02, 0.05, 0.1 and 0.2) and two modulus ratios (E_1/E_2 = 2.0 and 7.0) in linear and logarithm coordinates, respectively. From Fig. 7(a) and (c), it can be observed that given a crack spacing, a thicker coating layer corresponds to a lower threshold load, meanwhile a stiffer coating layer (with a larger Young's modulus) also accords to a lower threshold load compared to those with a lower stiffness. These observations are in an agreement with those of interfacial stresses predicted above: thicker and stiffer coating layers result in not only the higher interfacial shear and normal stresses (typically responsible for debonding failure) but also a lower resistance to progressive cracking in the coating layers. The latter can be understood in the view of the principle of energy conservation such that highly stressed stiff, thick surface layers would provide sufficient strain energy release to maintain the spontaneous crack growth. This conclusion also holds for surface coatings on curved substrates such as circular torsion shafts (Wu et al., 2008). Thus, the present research also indicates that ultrathin hard surface coatings (e.g., ultrathin diamond films used for cutting tools) are favorable to resist surface cracking. In addition, Fig. 7(b) and (d) indicates that there exists a simple linear relationship between the logarithm dimensionless critical load $\ln[p_0h_2^2/(G_ch_1)]$ and logarithm cracking spacing $\ln(L/h_2)$:

$$\ln[p_0h_2^2/(G_{Ic}h_1)] \approx -\frac{3}{2}\ln(L/h_2) + C, \tag{31}$$

where C is a constant. This scaling law largely agrees with that predicted by using bond-network model (Handge et al., 2000) and statistical models (Andersons et al., 2000, 2007), and is also close to the recent experimental observations (Ahmed et al., 2011; Bao et al., 2013).

In reality, the failure mode observed in actual surface coatings is a result of several competing factors relating the materials and external loads. For instance, interfacial debonding is a common failure mode in surface coating systems with weak interface strength. Also, it needs to be mentioned that the actual cracking phenomenon in surface coatings is much more complex than the idealized case as studied in work. In the above, we only phenomenologically adopted the concept of ERR G_c, which is a material property depending upon the crack mode in measurements. Moreover, this study has revealed the general planar stress state in a coating layer, thus the through-thickness cracking in the coating layer is actually mixed-mode with varying crack-mode mixture ratio; therefore, the corresponding G_c used for crack growth criterion should also be mode-mixture ratio dependent. As a simple strain energy approach, the ERR G_c adopted in this work can be understood as an average value.

4. Concluding remarks

In this study, semi-analytic solutions have been formulated for the interfacial free-edge stresses and progressive cracking criterion of hard coating systems subjected to tensile traction, bending moment, or/and temperature change. Within the framework of LEFM, a phenomenological strain energy criterion for progressive cracking in surface coatings has been established. This failure criterion has been demonstrated in predicting the density of progressive cracking in surface coating layers. Effects of thickness and modulus ratios on the free-edge stress distribution and the spacing of progressive cracking have been examined. The results gained in the present study indicate that coating layers of larger thickness and modulus are more pliant to cracking than those of thinner and compliant coating layers. Thus, the present model provides informative guidelines useful to rational surface coating design and cracking prediction, specifically for quantitative comparison between different coating systems.

Appendix A

The elements of matrix [A], [B], [C] and {D} are determined by the principle of minimum complementary strain energy of the coating system (Wu and Jenson, 2011) as follows

$$A_{11} = \frac{1}{105}(h_{12}^3 + e_{12}), \tag{A1}$$

$$A_{12} = \frac{11}{210}(h_{12}^2 - e_{12}), \tag{A2}$$

$$A_{22} = \frac{13}{35}(h_{12} + e_{12}), \tag{A3}$$

$$B_{11} = -\frac{4}{15}(h_{12} + e_{12}), \tag{A4}$$

$$B_{12} = \frac{1}{5}\{-[1 - 5\upsilon_1/(1-\upsilon_1)] + [1 - 5\upsilon_2/(1-\upsilon_2)e_{12}]\}, \tag{A5}$$

$$B_{22} = -\frac{12}{5}\left(h_{12}^{-1} + e_{12}\right), \tag{A6}$$

$$C_{11} = 4(h_{12}^{-1} + e_{12}), \tag{A7}$$

$$C_{12} = 6(h_{12}^{-2} - e_{12}), \tag{A8}$$

$$C_{22} = 12(h_{12}^{-3} + e_{12}), \tag{A9}$$

$$D_1 = \begin{cases} e_{12} - \frac{6M_0}{p_0 h_2^2} - \frac{1}{2p_0}[\alpha_1(1+\upsilon_1) - \alpha_2(1+\upsilon_2)]\Delta T E_1/(1-\upsilon_1^2) \\ \quad \text{(for combined mechanical and thermal loads)} \\ e_{12} - \frac{6M_0}{p_0 h_2^2} \text{ (for pure mechanical load)} \\ \quad -\frac{1}{2p_0}[\alpha_1(1+\upsilon_1) - \alpha_2(1+\upsilon_2)]\Delta T E_1/(1-\upsilon_1^2) \\ \quad \text{(for pure thermal load)} \end{cases} \tag{A10}$$

$$D_2 = \begin{cases} e_{12}\frac{12M_0}{p_0 h_2^2}, \text{ (for pure mechananical or combined} \\ \qquad \text{mechanical and thermal loads)} \\ 0, \text{ (for pure thermal load)} \end{cases} \tag{A11}$$

$$h_{12} = h_1/h_2, \tag{A12}$$

$$e_{12} = [E_1/(1-\upsilon_1^2)]/[E_2/(1-\upsilon_2^2)]. \tag{A13}$$

References

Ahmed, F., Bayerlein, K., Rosiwal, S.M., Göken, M., Durst, K., 2011. Stress evolution and cracking of crystalline diamond thin films on ductile titanium substrate: analysis by micro-Raman spectroscopy and analytical modelling. Acta Mater. 59, 5422–5433.

Andersons, J., Handge, U.A., Sokolov, I.M., Blumen, A., 2000. Analysis of brittle coating fragmentation under uniaxial tension for Weibull strength distribution. Eur. Phys. J. B 17, 261–268.

Andersons, J., Leterrier, Y., Tomare, G., Dumont, P., Månson, J.A.E., 2007. Evaluation of interfacial stress transfer efficiency by coating fragmentation test. Mech. Mater. 39, 834–844.

Bai, T., Pollard, D.D., 2000. Fracture spacing in layered rocks: a new explanation based on the stress transition. J. Struct. Geology 22, 43–57.

Bai, T., Pollard, D.D., Gao, H., 2000. Explanation for fracture spacing in layered materials. Nature 403, 753–756.

Bao, C.Y., Tang, C.A., Cai, M., Tang, S.B., 2013. Spacing and failure mechanism of edge fracture in two-layered materials. Int. J. Fract. 181, 241–255.

Bažant, Z.P., 1986. Mechanics of distributed cracking. Appl. Mech. Rev. 39, 675–705.

Bohn, S., Pauchard, L., Couder, Y., 2005a. Hierarchical crack pattern as formed by successive domain divisions. I. Temporal and geometrical hierarchy. Phys. Rev. E 71, 046214.

Bohn, S., Platkiewicz, J., Andreotti, B., Adda-Bedia, M., Couder, Y., 2005b. Hierarchical crack pattern as formed by successive domain division. II. From disordered to deterministic behavior. Phys. Rev. E 71, 046215.

Colina, H., Roux, S., 2000. Experimental model of cracking induced by drying shrinkage. Eur. Phys. J. E 1, 189–194.

Cox, H.L., 1952. The elasticity and strength of paper and other fibrous materials. Br. J. Phys. 3, 72–79.

Dufresne, E.R., Stark, D.J., Greenblatt, N.A., Cheng, J.X., Hutchinson, J.W., Mahadevan, L., Weitz, D.A., 2006. Dynamics of fracture in drying suspensions. Langmuir 22, 7144–7147.

Evans, A.G., Mumm, D.R., Hutchinson, J.W., Meier, G.H., Pettit, F.S., 2001. Mechanisms controlling the durability of thermal barrier coatings. Prog. Mater. Sci. 46, 505–553.

Handge, U.A., Sokolov, I.M., Blumen, A., 2000. Universal scaling and nonlinearity in surface layer fragmentation. Phys. Rev. E 61, 3216–3219.

Hong, A.P., Li, Y.N., Bazant, P.B., 1997. Theory of cracking spacing in concrete pavements. J. Eng. Mech. 123, 267–275.

Hutchinson, J.W., Suo, Z., 1992. Mixed mode cracking in layered materials. Adv. Appl. Mech. 29, 63–191.

Jenson, R.A., 2011. Stress-Function Variation Method and Its Applications in the Stress Analysis of Bonded Joints and Hard Coatings (M.S. thesis). North Dakota State University, Fargo, North Dakota, USA.

Kim, S.R., Nairn, J.A., 2000a. Fracture mechanics analysis of coating/substrate systems Part I: analysis of tensile and bending experiments. Eng. Fract. Mech. 65, 573–593.

Kim, S.R., Nairn, J.A., 2000b. Fracture mechanics analysis of coating/substrate systems Part II: experiments in bending. Eng. Fract. Mech. 65, 595–607.

Lee, W.P., Routh, A.F., 2004. Why do drying films crack. Langmuir 20, 9885–9888.

Leung, K.T., Jozsa, L., Ravasz, M., Neda, Z., 2001. Pattern formation-spiral cracks without twisting. Nature 410, 166–167.

Mal, D., Sinha, S., Mitra, S., Tarafdar, S., 2005. Formation of crack networks in drying laponite films. Physica A 346, 110–115.

Mei, H.X., Landis, C.M., Huang, R., 2011. Concomitant wrinkling and buckle-delamination of elastic thin films on compliant substrates. Mech. Mater. 43, 627–642.

Mishnaevsky Jr., L.L., Gross, D., 2005. Deformation and failure in thin films/substrate systems: methods of theoretical analysis. Appl. Mech. Rev. 58, 338–353.

Mizuguchi, T., Nishimoto, A., Kitsunezaki, S., Yamazaki, Y., Aoki, I., 2005. Directional crack propagation of granular water systems. Phys. Rev. E 71, 056122.

Nakahara, A., Matsuo, Y., 2006. Transition in the pattern of cracks resulting from memory effects in paste. Phys. Rev. E 74, 045102.

Neda, Z., Keung, K.T., Jozsa, K., Ravasz, M., 2002. Spiral cracks by drying precipitates. Phys. Rev. Lett. 88, 095502.

Singh, K.B., Tirumkudulu, M.S., 2007. Cracking in drying colloidal films. Phys. Rev. Lett. 98, 218302.

Thouless, M.D., 1990. Crack spacing in brittle films on elastic substrates. J. Am. Ceram. Soc. 73, 2144–2146.

Timoshenko, S., Goodier, J.N., 1951. Theory of Elasticity, second ed. McGraw-Hill, New York, USA.

Wu, X.F., Jenson, R.A., 2011. Stress-function variational method for stress analysis of bonded joints under mechanical and thermal loads. Int. J. Eng. Sci. 49, 279–294.

Wu, X.F., Zhao, Y.H., 2013. Stress-function variational method for interfacial stress analysis of adhesively bonded joints. Int. J. Solids Struct. 50, 4305–4319.

Wu, X.F., Dzenis, Y.A., Strabala, K.W., 2008. Free-edge stresses and progressive cracking in surface coatings of circular torsion bars. Int. J. Solids. Struct. 45, 2251–2264.

Xia, Z.C., Hutchinson, J.W., 2000. Crack patterns in thin films. J. Mech. Phys. Solids 48, 1107–1131.